

Study of the bandwidth of an integrated micro-transformer

M. A. Taha^{1,2}, A. Abderahim^{1,3}, O. B. Arafat^{1,2}, S. Capraro¹, P. David¹, and J. J. Rousseau¹

¹LabHC UMR 5516, CNRS, 42023 Saint-Etienne, JEAN MONNET University of Saint-Etienne, Saint-Etienne, France

²Departement of Electrical Engineering, National Institute of Science and Technology of Abeche, Abeche, Chad

³Departement of Science and Technology Department, University of N'Djamena, N'Djamena, Chad

Copyright © 2021 ISSR Journals. This is an open access article distributed under the *Creative Commons Attribution License*, which permits unrestricted use, distribution, and reproduction in any medium, provided the original work is properly cited.

ABSTRACT: This paper presents a study on the main characteristics of an integrated transformer i.e. the low and high cut-off frequencies (F_{CL} and F_{CH}) and the voltage gain within the bandwidth (G_0). After a description of the integrated transformer and its micro-fabrication, the measured transformer frequency response is given. An equivalent circuit is derived and the method to determine each element is shortly described. Then, the paper focuses on the influence of geometrical dimensions and a few characteristics of materials on the low and high cut-off frequencies (F_{CL} and F_{CH}) and on the voltage gain (G_0). An analytical expression is derived for F_{CL} , F_{CH} and G_0 . The aim of this article is to identify the main parameters that limit the bandwidth and the voltage gain.

KEYWORDS: Integrated transformer, bandwidth, cut-off frequencies, gain.

1 INTRODUCTION

In the field of embedded devices, the development of integrated magnetic components is essential to reduce both sizes and weight. Different approaches have been used for design and micro-fabrication of integrated magnetic components such as inductors and transformers:

- Numerous magnetic components were studied for very high frequencies between some tens of MHz and 1GHz. Such components do not use magnetic material [1], [2].
- Magnetic materials are used in order to increase inductance values or to reduce sizes but such devices are classically used at low frequency [3], [4].

We studied and micro-fabricated an integrated transformer with ferrite material [5]. This component which exhibits low sizes is fabricated with different stacked layers on a glass mechanical substrate: Yttrium Iron Garnet (YIG) ferrite for magnetic layers, spiral conductors in copper, insulator layer using SU8 epoxy-based negative photoresist.

Design and simulations were performed by using a commercial finite element method solver (HFSS). Characterizations were carried out with both impedance meter and Vector Network Analyzer (VNA).

The aim of this article is to discuss about the main characteristics of this transformer and their limits, i.e. low and high cut-off frequencies and the gain in bandwidth. Two approaches have been defined for this study:

- With the help of measurements using a VNA and simulations performed with HFSS, an equivalent circuit was defined and the equivalent circuit parameters have been determined. In this article, the influence of each parameter is studied in order to simplify the equivalent circuit in different frequency domain. An analytical expression is derived for cut-off frequencies and for gain.
- Simulations carried out with HFSS by changing geometric parameters and main characteristics of materials allow validating our results.

In the second paragraph, we give some information on the design and constitution of the transformer. Characterizations with low amplitude sinusoidal excitation are given as well. An equivalent circuit is defined in the third paragraph: the equivalent circuit is presented together with the parameter determination method. The two following paragraphs concern the bandwidth study depending on certain parameters of the transformer. The influence of some parameters on the low and high cut-off frequencies is discussed. The paragraph VI is about the voltage Gain G_0 of the no-load transformer.

2 INTEGRATED TRANSFORMER FABRICATION

2.1 DEVICE DESCRIPTION AND MICRO-FABRICATION

The transformer is intended for driving power switches such as IGBT, Power MOSFET [6], [7], [8]. It was designed for a high coupling factor between primary and secondary windings, a high magnetizing inductance and a low coupling capacitance between primary and secondary windings.

The micro-fabricated transformer shown Fig. 1 is made with several stacked layers, insulator layer using SU8 epoxy-based negative photoresist, conductor layer based on copper and magnetic layer based on ferrite material. The transformer consists in two parts: Primary and secondary parts of the transformer are almost identical, which are separately fabricated. Each part is composed of:

- a mechanical glass substrate which can be removed at the end of the fabrication if necessary.
- a magnetic substrate with a thickness between 300 and 1000 μm in various designs
- a coil made in copper
- an air-bridge to connect inner pad to the outer one

Finally, the two part are gluing assembled.

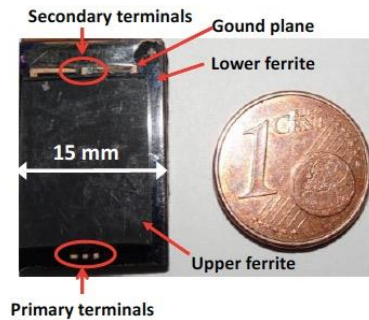


Fig. 1. Photograph of Face to Face transformer

Fig. 2 and illustrate the main geometrical dimensions of the transformer. The two coils exhibit the same number of turns $n_1=n_2=15$ and are rotated by 45°.

In order to bury copper conductors inside the magnetic material, a laser Femtosecond laser micromachining was used. Copper deposition was performed by RF sputtering, followed by a step of photolithography and wet etching to obtain the spiral coil. In order to connect central pad to the outer pad an air-bridge was added by using the same previous steps insulator and copper deposition photolithography and wet etching). Fig. 3 shows a cross section of the transformer.

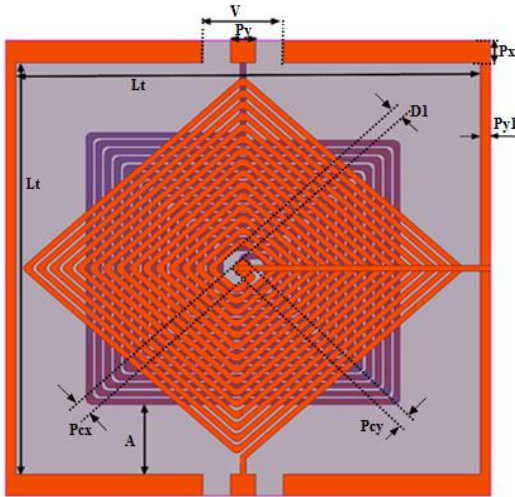


Fig. 2. Top view of the transformer [10]

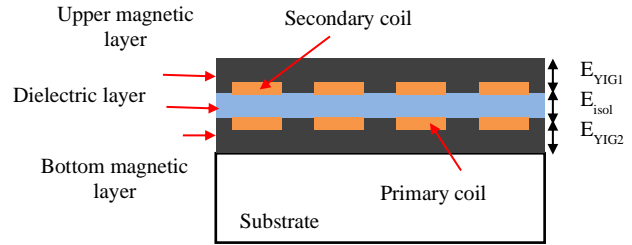


Fig. 3. Cross section of the transformer with primary and secondary coils buried in magnetic cores

Table 1. Transformer parameters [10]

N	Winding turn	15
w	Copper ribbon width	125 μm
D	Distance between turns	60 μm
D1	Distance between the central pad and the first turn	400 μm
A	Distance between the outside turn and the ground plane	1600 μm
V	Distance between ground plane	800 μm
Px=Py	Length and width of the outside pad	500 μm
PcX=PcY	Length and width of the central pad	300 μm
Py1	Width of the ground plane	200 μm
L _T	Device length $L_T=2*(A+D1+N*W+(N-1)*D)$	9430 μm
e _{co}	Conductor thickness	30 μm
E _{insul}	Dielectric thickness	30 – 95 μm
E _{YIG1} =E _{YIG2}	Magnetic material thickness	300 – 1000 μm

2.2 AC CHARACTERIZATION

Measurements have been carried out to determine the transformer bandwidth and to compare these results with those obtained by simulation.

The frequency response of the transformer was measured by using the set-up defined Fig. 4.

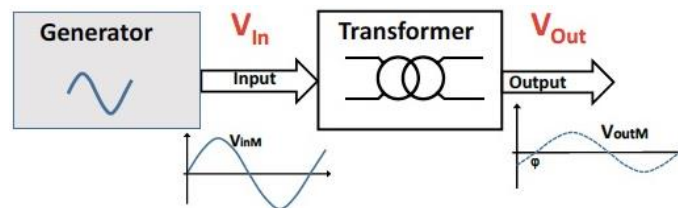


Fig. 4. Measurement set-up

The primary winding is supplied with a low amplitude sinusoidal waveform corresponding to a classical no-load transformer test. Both primary and secondary voltages are measured with an oscilloscope. The visualization of the two signal waveforms allows to control that all signals remain sinusoidal.

Fig. 5 shows the frequency response: (V_{out}/V_{in}) dB versus frequency. The bandwidth is defined at ± 3 dB and ranges from 20kHz to 7MHz. The low cut-off frequency (f_{CL}) is equal to 20kHz while the high cut-off frequency (f_{CH}) reaches 7MHz. The gain G_0 of the transformer, without any load, is equal to 0.86. One can also observe a resonance around 15MHz.

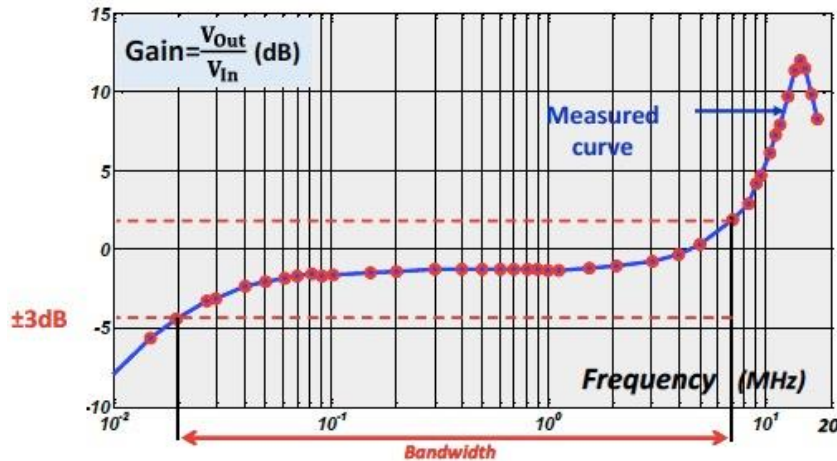


Fig. 5. Frequency response of the transformer [9]

The influence of both geometrical dimensions and main characteristics of materials on the main characteristics of the transformer will be studied in the next paragraph.

3 EQUIVALENT CIRCUIT

In order to determine which geometrical or physical parameters have an impact on the main characteristics of the transformer i.e. the cut-off frequencies (f_{CL} and f_{CH}) and the Gain G_0 , the following steps should be performed:

Step 1:

- Define an equivalent circuit for the transformer,
- Identify each element of the equivalent circuit.

Step 2:

For each main characteristic f_{CL} , f_{CH} and G_0

- Study the influence of each equivalent circuit parameter by using a simulation tool,
- Simplify the equivalent circuit for each frequency domain,
- Determine an analytical expression of f_{CL} , f_{CH} and G_0 ,
- Study the impact of some dimensions and main characteristics of materials.

3.1 EQUIVALENT CIRCUIT

An electrical model has been defined (Fig. 6) in order to take into account the losses of the magnetic material according to the frequency (R_f), the coupling between turns and ground plane (C_1 and C_2), the proximity and skin effects in the conductors (r_1 and r_2), and the coupling between primary and secondary inductors (C_{12}).

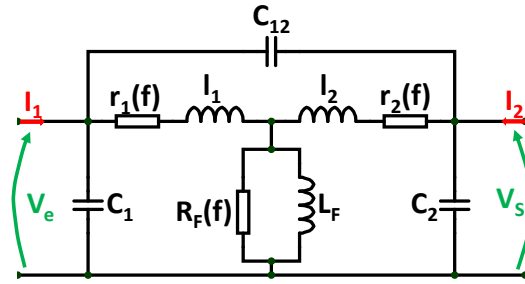


Fig. 6. Electrical model of the transformer [10]

3.2 IDENTIFICATION OF EQUIVALENT CIRCUIT ELEMENTS

In order to extract these parameters, it is considered that the transformer will not operate beyond 50 MHz. Under these conditions and according to the magnetic material properties, where the relative permeability is constant up to these frequencies, we can consider that l_1 , l_2 and L_F are constant over the broad band frequency. One the other, we consider that capacitances C_1 , C_2 and C_{12} are independent of the frequency.

So as to extract these different elements, it is necessary to use impedance and admittance matrices obtained by measurements. The method to obtain parameters are summarized on table 2.

Table 2. Transformer parameters extraction [10]

Parameter	Matrix element	Extraction
r_1 and r_2	Z_{11} , Y_{11} and Y_{12}	Amplitude of the resonance
L_{F0}	Z_{12}	Slope of 20dB/dec
l_{10}	Y_{11} and Y_{12}	Slope of 20dB/dec
l_{20}	Y_{12}	Slope of 20dB/dec
C_{12}	Y_{12}	At the resonance
C_1	Y_{11}	At the resonance
C_2	Y_{22}	At the resonance

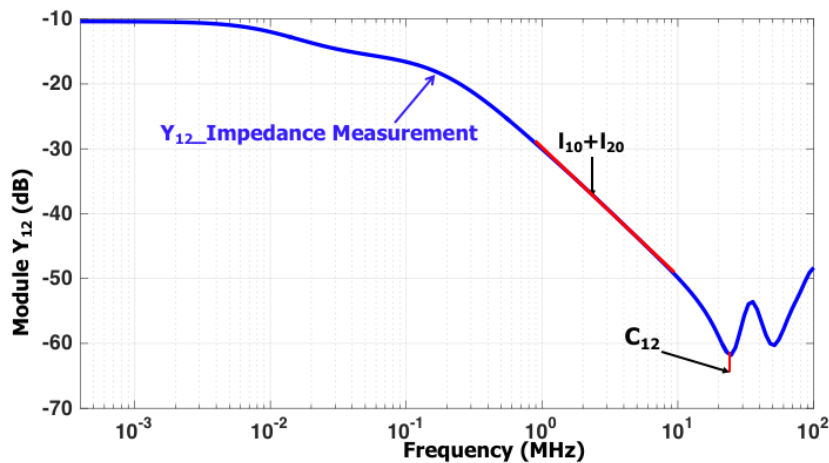


Fig. 7. Y_{12} parameter versus frequency

An example of the extraction of l_{10} , l_{20} and C_{12} is given in figure 7 where the extraction of l_{10} and l_{20} are obtained by the slope of Y_{12} parameter for lower frequencies and the C_{12} parameter is obtained at the resonance frequency.

4 THE LOW CUT-OFF FREQUENCY f_{CL}

In this paragraph, the influence of two equivalent circuit elements (r_1 and L_F), of a geometrical dimension (E_{insu}) and of a material characteristic (μ_r) is studied.

4.1 STUDY OF LOW CUT-OFF FREQUENCY VERSUS EQUIVALENT CIRCUIT ELEMENTS.

At low frequency, the three capacitors C_1 , C_2 and C_{12} can be neglected. If no load is connected to the secondary winding the secondary winding impedance does not impact low cut-off frequency [16]. Moreover, the core losses at low frequency are weak, that means the resistance R_F is very high and is neglected. Then simplified model suggested by Chris Trask [13], [14] is well suitable to describe the transformer behavior at low frequency.

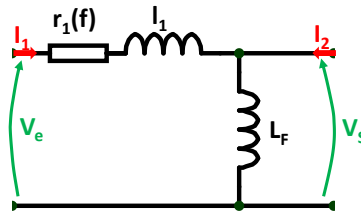


Fig. 8. Simplified model at low frequency

Then, only three elements define the low-cut frequency of the transformer as shown Fig. 8: the primary leakage inductance l_1 , the magnetizing inductance L_F and the primary winding resistance r_1 . The low cut-off frequency is expressed as follows:

$$f_{CL} = \frac{1}{2\pi * \tau_2} = \frac{1}{2 * \pi * \left(\frac{L_F + l_1}{r_1}\right)} \quad (1)$$

Some simulations are performed to illustrate the influence of these three elements:

4.1.1 INFLUENCE OF THE RESISTANCE R_1

At low frequency, both skin effect and proximity effect can be neglected, then the primary winding resistance is independent of frequency. This resistance only depends on the material resistivity ρ and the conductor dimensions (length l , width w and thickness e) [15].

$$R = \rho \frac{L}{l * e} \quad (2)$$

Fig. 9 shows the evolution of the frequency response for different values of the resistance which ranges from 1.5 to 6 Ω , the nominal value for the fabricated transformers is around 2 Ω . These simulations are performed with the equivalent circuit shown Fig. 6.

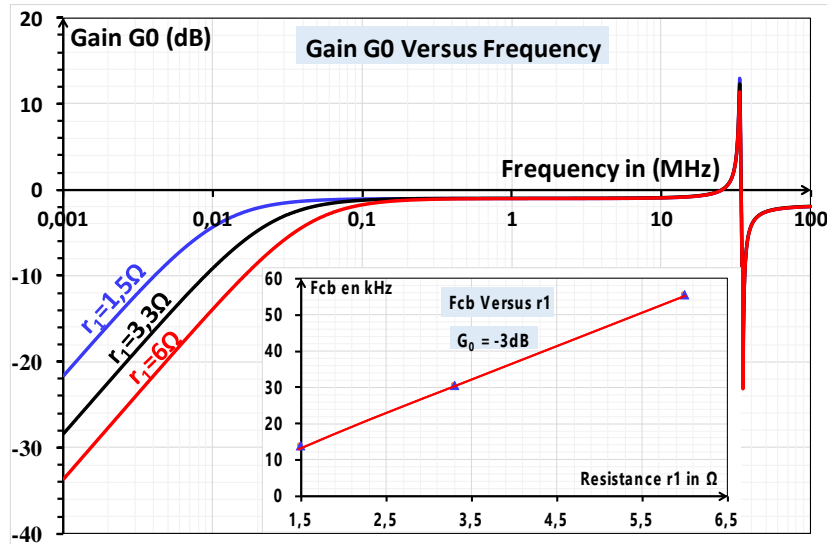


Fig. 9. Influence of the resistance r_1 of the low cut-off frequency

The low cut-frequency linearly increases with the resistance r_1 as given by equation (1).

4.1.2 INFLUENCE OF THE MAGNETIZING INDUCTANCE L_F

The effect of the magnetizing inductance L_F on the low cut-off frequency F_{CL} is shown on Fig. 10. The same approach is implemented using the electrical model shown Fig. 6. For these simulations the magnetizing inductance ranges from 20 μH to 30 μH (the typical value for the fabricated transformer is around 15 μH).

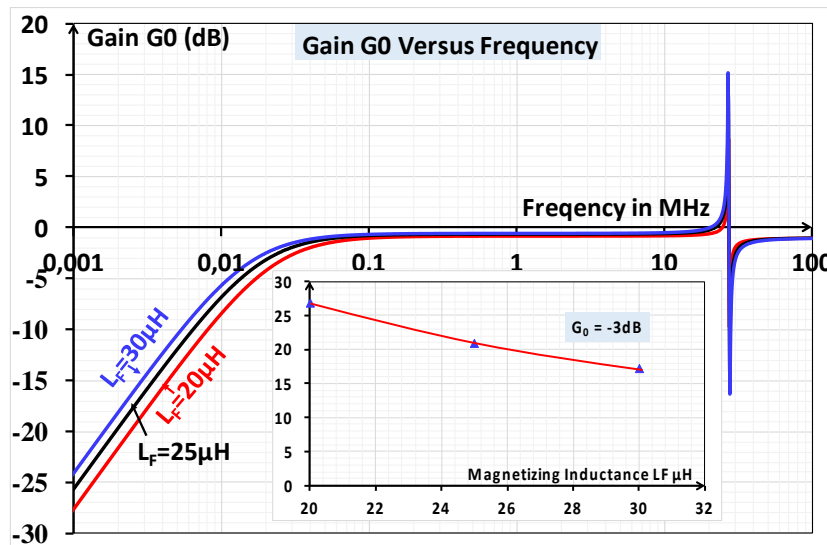


Fig. 10. Influence of L_F on the cut-off frequency (F_{CL})

As expected, the low cut-off frequency decreases when the increasing of magnetizing inductance.

4.2 STUDY OF LOW CUT-OFF FREQUENCY VERSUS GEOMETRICAL AND PHYSICAL PARAMETERS OF THE TRANSFORMER

In order to confirm these results, different simulations are performed using HFSS software. Two of them are shown below, the first one concerns the influence of the air-gap and the second one is related to the permeability of the magnetic material.

4.2.1 INFLUENCE OF THE AIR-GAP THICKNESS ON THE LOW CUT-OFF FREQUENCY FCL

The air-gap between the two magnetic layers corresponds to the insulator layer made with the SU8 photoresist as shown on Fig.3 [10]. This SU8 layer insures a working insulation voltage around 100 V per some μm . Fig. 11 shows the effect of this air-gap on the low cut-off frequency. By increasing the SU8 thickness between 15 and 50 μm , one can observe that the cut-off frequency increases due to the decrease of the magnetizing inductance.

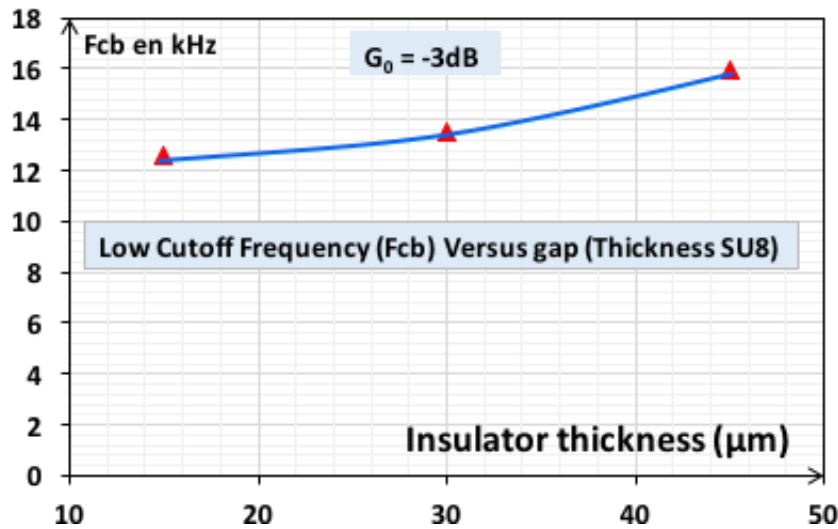


Fig. 11. Influence of the insulator thickness on the low cut-off frequency

4.2.2 INFLUENCE OF THE RELATIVE PERMEABILITY μ_r ON THE LOW CUT-OFF FREQUENCY FCL

In this paragraph the influence of the magnetic material relative permeability is studied. For high frequency ferrite such as Yttrium Iron Garnet the relative permeability is quite low, classically less than 100. Fig. 12 shows the evolution of F_{CL} versus the relative permeability μ_r . One can see that as the permeability rises, the cut-off frequency decreases. Indeed, if the permeability μ_r increases the magnetizing inductance L_F increases as well. In these conditions, the cut-off frequency F_{CL} decreases as given by equation (1).

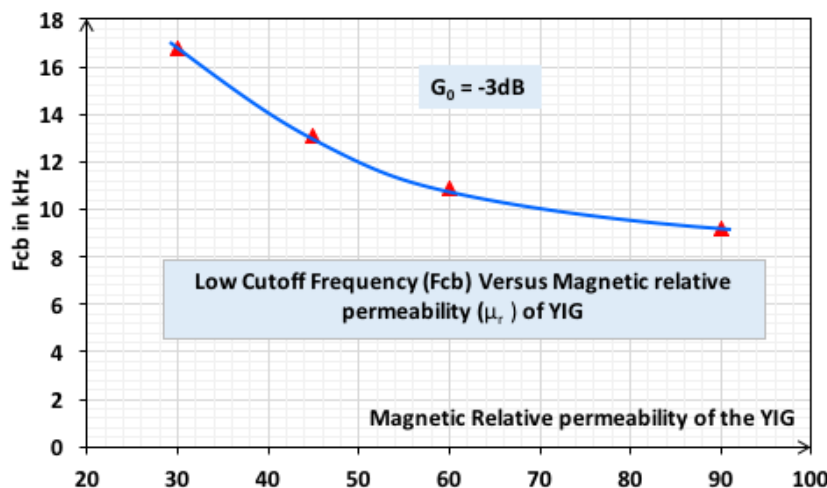


Fig. 12. Influence of the permeability μ_r on F_{CL}

As a conclusion, one can say that the low cut-off frequency F_{CL} only depends on three parameters of the equivalent circuit: the resistance of the primary winding r_1 , the magnetizing inductance L_F and the leakage inductance l_1 of the transformer primary. In order to decrease this low cut-off frequency, one can exploit several geometrical and physical parameters such as conductor dimensions, insulator thickness, relative permeability ...

5 THE HIGH CUT-OFF FREQUENCY F_{CH} .

In this paragraph, the influence of one equivalent circuit element (C_{12}) and of a geometrical dimension (E_{insu}) is considered.

5.1 STUDY OF HIGH CUT-OFF FREQUENCY F_{CH}

At high frequency, the resistances r_1 and r_2 are neglected in comparison with the impedance l_1w et l_2w . The capacitor C_1 , in parallel with the primary winding do not affect the high cut-off frequency. Then, the equivalent circuit shown in Fig. 13a is used to determine F_{CH} . By using the Kennelly's Star-Delta Transformation, the circuit shown in Fig. 13b is obtained. The expression of the three inductances L_{AB} , L_{AC} and L_{BC} are the following:

$$L_{AB} = \frac{l_1 \times l_2 + l_2 \times L_F + L_F \times l_1}{L_F} \quad (3)$$

$$L_{BC} = \frac{l_1 \times l_2 + l_2 \times L_F + L_F \times l_1}{l_1} \quad (4)$$

$$L_{AC} = \frac{l_1 \times l_2 + l_2 \times L_F + L_F \times l_1}{l_2} \quad (5)$$

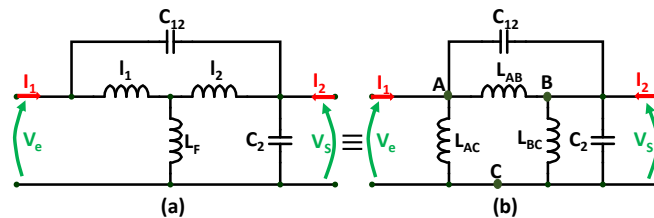


Fig. 13. Kennelly's Star-Delta Transformation: a) Star, b) Delta

The equivalent circuit shown in Fig. 3 is used to simulate the behavior of the transformer at medium and high frequencies as shown in Fig. 14. One can see that resonance frequency and high cut-off frequency are very close. An acceptable approximation is to consider $F_{CH}=F_{reso}$. In these conditions, an expression of high cut-off frequency is:

$$F_{CH} \approx F_{reso} = \frac{1}{2 \times \pi \times \sqrt{\left(\frac{L_{AB} \times L_{BC}}{L_{AB} + L_{BC}}\right) \times (C_{12} + C_2)}} \quad (6)$$

The resonance is due to the inductances L_{AB} in parallel with L_{BC} and the capacitances C_{12} in parallel with C_2 .

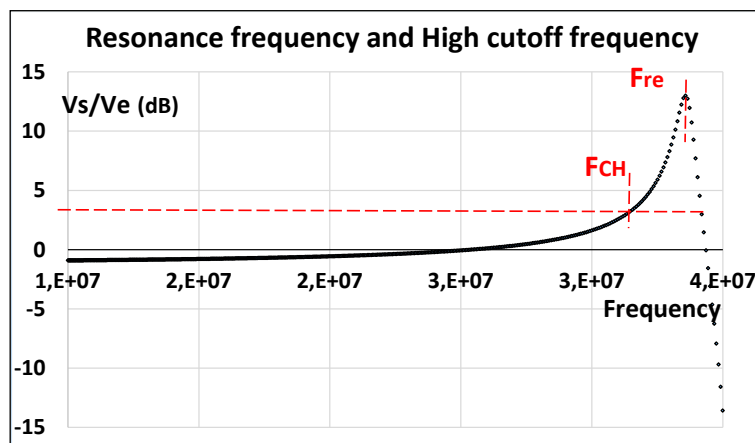


Fig. 14. Resonance and high cutoff frequencies

In order to validate this approximation, we compare in Fig. 15 the resonance frequency calculated with the formula (6) and the high cut-off frequency determined by simulation with the electrical circuit given in Fig. 3. For a capacitance C_{12} ranging from 6 to 9 pF, there is not significant difference between these two frequencies.

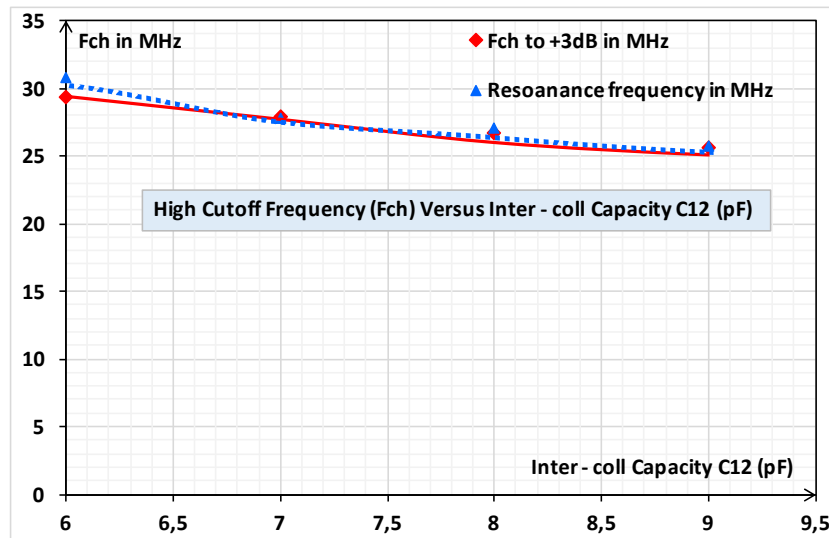


Fig. 15. Influence of C_{12}

5.2 STUDY OF HIGH CUT-OFF FREQUENCY VERSUS SU8 THICKNESS

In order to confirm this result, different simulations are performed using HFSS software. The capacitance C_{12} depends on the insulator thickness between the two magnetic layers. An approximate formula for C_{12} is given using the formula of parallel plate capacitor. For this case d is equal to the insulator thickness E_{insu} .

$$C = \epsilon_0 \epsilon_r \frac{S}{d} \quad (7)$$

Thus, by simulation we varied the insulator thickness to study its influence on the high cut-off frequency. Fig. 16 shows the evolution of F_{CH} versus E_{insu} which ranges from $15\mu m$ to $45\mu m$. The capacitance decreases when the insulator thickness E_{insu} increases. For low thickness, the total capacitance $C_{12}+C_2$ decreases and the cut-off frequency increases as expected. But, for high thickness, the capacitance C_{12} becomes low and the total capacitance $C_{12}+C_2$ remains quite constant, the cut-off frequency does significantly not change.

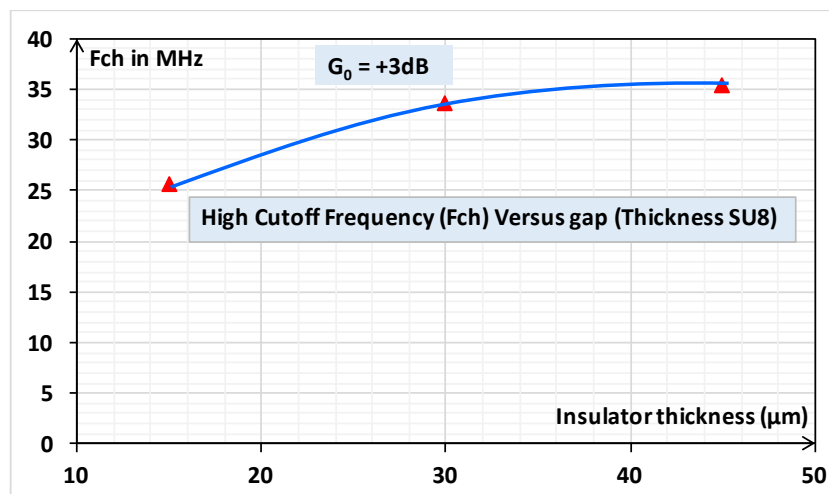


Fig. 16. High cut-off frequency F_{CH} versus insulator thickness E_{insu}

In conclusion, the interwinding capacitance C_{12} , which is greater than C_2 limits the bandwidth of the transformer. Moreover, for switch drivers, C_{12} must to be decreased as low as possible (few pF) [17].

6 THE GAIN G_0

The Gain G_0 is the ratio between the secondary voltage V_s over the primary one for no load. This Gain is defined within the bandwidth.

$$G_0 = \frac{V_s}{V_e (i_s=0)}$$

In these conditions, one can simplified the equivalent circuit given in Fig. 6: Capacitors are removed and the secondary impedance as well (no load is connected) as shown Fig. 17.

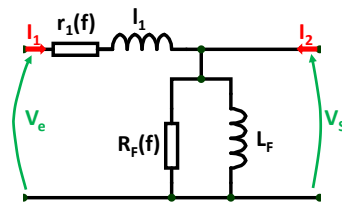


Fig. 17. Equivalent circuit within the bandwidth

Classically for these frequencies within the bandwidth, the resistance r_1 is much smaller than the impedance $l_1\omega$ ($r_1 \ll j l_1\omega$) and the resistance R_r is greater than $L_F\omega$ ($R_r \gg j L_F\omega$) [14]. Thus, using voltage divider rule, the gain G_0 is expressed as follows:

$$G_0 = \frac{L_F}{L_F + l_1} = \frac{1}{1 + \frac{l_1}{L_F}} \quad (8)$$

Thus, the gain G_0 only depends on the ratio between the magnetizing inductance L_F and the leakage inductance l_1 [15]. A simulation with the complete electrical model given in Fig. 6 was performed and the results shown Fig. 17, are compared to those obtained using formula (8).

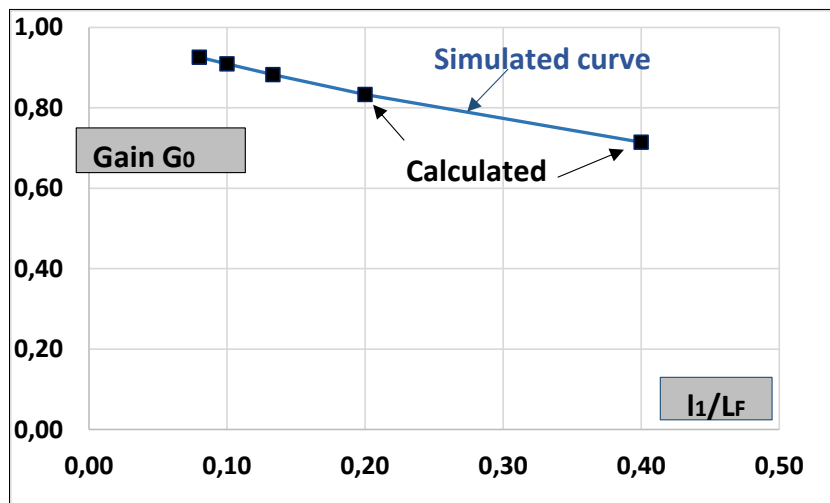


Fig. 18. Gain G_0 versus the ratio l_1/L_F

One can observe that the results given by the two approaches are identical. For a low ratio of l_1/L_F i.e. with few leakage flux, the Gain G_0 tends towards the maximum value equals to 1 ($n_1=n_2$). Conversely, a bad coupling between primary and secondary windings leads to decrease the gain.

- In order to confirm these results, simulations were performed by using HFSS. The influence of two parameters were studied: the insulator thickness between primary and secondary windings
- the magnetic material permeability μ_r .

Fig. 19 illustrates the influence of the insulator thickness on the Gain G_0 for reasonable thicknesses that ranges between 15 and 45 μm . The increase of insulator thickness leads to a less good coupling between windings, which causes an increase of the leakage inductance and a decrease of the magnetizing inductance.

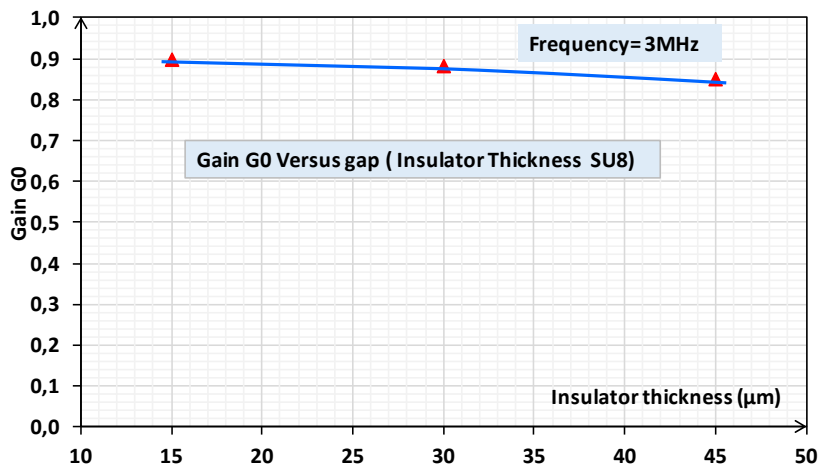


Fig. 19. Gain G_0 versus SU8 insulator thickness

- The next figure shows the influence of magnetic permeability on the Gain. The higher the magnetic permeability, the less the leakage flux are important, then, the ratio I_1/L_f increases and therefore the gain as well.

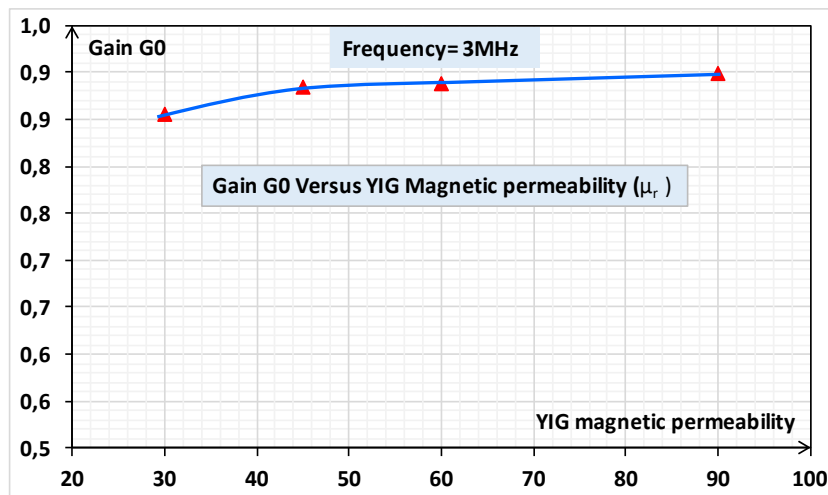


Fig. 20. Gain G_0 versus magnetic permeability μ_r

7 CONCLUSION

The aim of this article was to identify the main parameters that limit the bandwidth and the voltage gain of an integrated transformer. First of all, the integrated transformer and some information about its fabrication were presented. Thus, a equivalent circuit was defined and its parameters were determined by using measurements. A study of influence of each element of the equivalent circuit was carried out and the main results were presented. An expression of cut-off frequencies and Gain of the transformer was determined. Simulations using a circuit simulation software and a finite element software were performed to confirm our results.

REFERENCES

- [1] C.D. MEYER et al, "High-Inductance-Density, Air-Core, Power Inductors, and Transformers Designed for Operation at 100–500 MHz", *IEEE Transactions On Magnetics*, Vol. 46, pp.2236-2239, June 2010.
- [2] Rongxiang WU, S.Y. Huil, "A Novel Silicon-Embedded Coreless Transformer for Isolated DC-DC Converter Application", *IEEE Proceedings of the 23rd International Symposium on Power Semiconductor Devices & IC's*, pp.352-355, May 2011.
- [3] Hideyuki ITO et al, "Fabrication of Planar Power Inductor for Embedded Passives in LSI Package for Hundreds Megahertz Switching DC–DC Buck Converter", *IEEE Transactions On Magnetics*, Vol.47, pp.3204-3207, October 2011.
- [4] Ningning Wang, et al, "High Efficiency Si Integrated Micro-transformers Using Stacked Copper Windings for Power Conversion Applications", *IEEE Enterprise Ireland UTIM, PHMiS projects*, pp.411-416, 2012.
- [5] K. Youssouf, F. Kahlouche, M. Soultan, M. Youssouf, M.H. Bechir, S. Capraro, J.P. Chatelon, A. Sibli, J.J. Rousseau, "Design and study of interleaved and face to face magnetic microtransformers", *IEEE trans on electron devices*, vol. 61, pp. 2873-2878, August 2014.
- [6] Dejan VASIC, François COSTA, Emmanuel SARRAUTE, "A New MOSFET & IGBT Gate Drive Insulated By A Piezoelectric Transformer", *IEEE 32nd Annual Power Electronics Specialists Conference, 2001. PESC*, pp.1479-1484, Vol.3, 17-21 June 2001.
- [7] Ali Moazenzadeh, Fralett Suárez Sandoval, Nils Spengler, Vlad Badilita, "3-D Microtransformers for DC–DC On-Chip Power Conversion", *IEEE Transactions on Power Electronics*, Vol. 30, pp.5088-5102, 06 November 2014.
- [8] D.A. Frickey, "Conversions between S, Z, Y, H, ABCD and T parameters which are valid for complex source and load impedances", *IEEE Transactions on Microwave Theory and Techniques*, vol. 42, pp. 205-211, February 1994.
- [9] M. A. Taha, D. A. Oumar, A. Abderahim, S. Capraro, D. Pietroy, and J.J. Rousseau, "Simulation, Modeling, Manufacturing and Characterization of planar Magnetic Face to Face Integrated Transformer", *IEEE Transaction on Magnetics*, Vol. 54, october 2018.A.
- [10] T. Mahamat, B. Danoumbé, M. Youssouf, J. P. Chatelon, S. Capraro, and J.J. Rousseau, "Optimization of integrated magnetic planar transformer" in *Proc. Eur. Conf. Power Electron. Appl. (EPE)*, Karlsruhe, Germany, p1-8, Sep. 2016.
- [11] D. C. Laney, L. E. Larson, P. Chan, J. Malinowski, D. Haramé, S. Subbanna, R. Volant, et M. Case, "Lateral microwave transformers and inductors implemented in a Si/SiGe HBT process", in *Microwave Symposium Digest, 1999 IEEE MTT-S International*, vol. 3, p. 855-858, 1999.
- [12] Chris Trask, "Wideband Transformers: An Intuitive Approach to Models, Characterization and Design," *Applied Microwave & Wireless*, Vol. 13, No. 11, November 2001, pp. 30-41.
- [13] Chris Trask "Wideband Transformer Models: Measurement and Calculation of Reactive Elements", *earthlink.net*, 2008.
- [14] A. Abderahim, A. T. Mahamat, J. P. Chatelon, D. Pietroy, S. Capraro, and J. J. Rousseau, "Approach of copper losses determination in planar windings" *Electron. Lett.*, vol. 52, pp. 1050–1052, Jun. 2016.
- [15] Ningning Wang, Terence O'Donnell, Saibal Roy, Santosh Kulkarni, Paul Mccloskey, and Cian O'Mathuna, "Thin Film Microtransformer Integrated on Silicon for Signal Isolation", *IEEE Transactions on Magnetics*, Vol.. 43, No. 6, pp.2719-2721 June 2007.
- [16] John R. Long, "Monolithic Transformers for Silicon RF IC Design", *IEEE Journal Of Solid-State Circuits*, Vol. 35, No. 9, pp. 1368-1382, September 2000.
- [17] Aliakbar Ghadiri and Kambiz Moez, "Bandwidth Enhancement of On-Chip Transformers Using Negative Capacitance", *IEEE Transactions On Circuits And Systems—II: Express BriefsR*, Vol. 59, No. 10, pp.648-652, October 2012.